Coll. Antropol. **31** (2007) 2: 523–529
Original scientific paper

Blood Flow Multiscale Phenomena

Ante Agić[1], Budimir Mijović [2] and Tatjana Nikolić [3]

[1] Faculty of Chemical Engineering and Technology, University of Zagreb, Zagreb, Croatia
[2] Faculty of Textile Technology, University of Zagreb, Zagreb, Croatia
[3] University Clinic of Traumatology, University of Zagreb, Zagreb, Croatia

A B S T R A C T

The cardiovascular disease is one of most frequent cause deaths in modern society. The objective of this work is analyse the effect of dynamic vascular geometry (curvature, torsion,bifurcation) and pulsatile blood nature on secondary flow, wall shear stress and platelet deposition. The problem was examined as multi-scale physical phenomena using perturbation analysis and numerical modelling. The secondary flow determined as influence pulsatile pressure, vascular tube time-dependent bending and torsion on the main axial flow. Bifurcation and branching phenomena are analysed experimentally through, blood-like fluid pulsatile flow across elastic rubber-like Y-model model. The problem complex geometry near branching in platelet deposit modelling is resolved numerically as Falker-Skan flow.

Key words: *curved tube model, bifurcation flow, torsion, platelet deposition*

Introduction

Today it is accepted in medical community, that the development and progression of atherosclerosis is related with hemodynamics phenomena amang others. Blood flow studies are important for understanding the origin of vascular diseases, its diagnosis and treatments. Strong correlation between the sites of flow disturbance (velocity and shear stress field reduction with departs from unidirectional patterns) and the preferred sites for the genesis and development of vascular diseases clinically found in man[1]. Caro[1] considered hemodynamic factors to have a major role in the formation of plaques and thrombosis. Plaque formation at sites with such characteristic as curvatures, bifurcation, tortuosity and branching results in local wall shear stress (WSS) intensifaing the atherogenesis by inducting the vascular response of the endothelium. Unstaedy blood flow characteristics, rather than the magnitude of WSS per se, may be the major determinant of hemodynamically induced endothelial cell turnover, a precursor to plaque formation. Several papers[2,3] have reported about dominant geometric influence factors on unsteady flow; time-dependent curvature and torsion, different branching angles, and tube diameter ratio. Atherosclerotic plaques are developed predominantly at sites as bends and bifurcations, inside of curves, in regions where the arterial cross-section undergoes an expansion. There is still some debate on the causes of atherosclerosis, but there is evidence that initiated regions are correlated with the distribution of arterial wall shear stress and concentration of toxic materials. These plaques tend to develop in regions of low wall shear stress and in regions where the shear stress changes direction in the course in the cardiac cycle. Helical flow has a significant effect in mechanisms of endothelial damage repair and preventing plaque deposition[4]. Numerical simulation of pulsatile flow using the multiphase flow dynamics has also been performed through a realistic right coronary artery[5]. The multiscale numerical methods with blood as suspension of discrete particles are popular today[6]. According to Liu[7], local multiscale fluid-solid effects play a leading role in the localization of atherosclerosis in blood vessel, and can be solved by newly developed immersed finite element method. Mijovic[8] reported the nature of development of the shear stresses in elastic Y model under pulsatile flow conditions. Gammack and Hydon[9] theoretically studied unsteady flow in artery with non-uniform curvature and torsion. A general framework for pulsatile flow through thin-walled elastic vessel theoretically and numerically was done by Pontrelli[10].

In this study, we consider a flow driven by an oscillatory pressure gradient in vessels with time-dependent

Received for publication April 4, 2007

curvature and torsion. Local effects of branching are determined experimentaly by observation on a model. The platelet deposition and thrombus formation are analysed numericaly using Falker-Skan flow past a wedge near branching.

Materials and Methods

Multiscale phenomena

Hemodynamics is a multi-scale physical phenomena, different objects come in interaction and they together reveal the phenomena of living. At the macroscale, hemodynamics is characterized by the flow and pressure propagation in a multi-branching flexible network. System behaviour can be predicted efficently using one-dimensional equivalent model. The meso-hemodynamics treat the blood as multi-phase fluid suspension with strong interaction with deforming vascular wall, Figure 1. On the microscale level, we have microcirculation in the capillaries, with mass transport of blood cells, oxygen, and nutrient. At the cell level, the particle method is a natural choice for hemodynamics simulating toll. A new multiscale simulation technique that couples Navier-Stokes equations with generalized particle methods is developed. The solid-fluid interaction with immersed methodology distributes nanoscale effects in macroscale fluid domain[7]. Some phenomena such as multiparticle adhesive and cohesive dynamics method are used in generalized particle methods. The each component of the blood is represented by an assembly of discrete particle. The system can reperesent as one particle/discrete object (e.g., a platelet) or a set particles representing physical domain[6] (e.g., red blood cell).

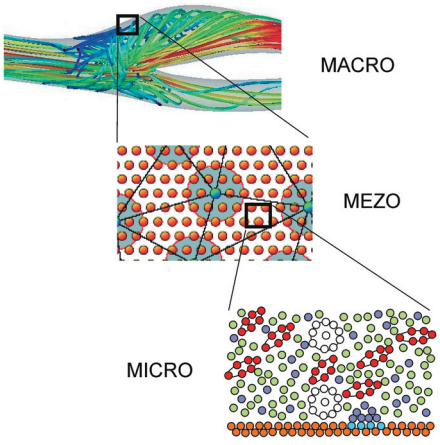

Fig. 1. Multiscale hemodynamics.

Branching and recirculation

At the level of global circulation system, hemodynamics is characterized by the flow and pressure propagation in a multi-branching 1D network with compliant and tapering vessels. The insight into some local phenomena such as branching, vessel curvature and torsion cannot be analysed by this global 1D circulation model. Therefore 3D model can be described by system of equations representing continuity of mass and momentum conservation. The blood incompressibility condition is described as

$$div\ v = 0 \tag{1}$$

The Navier-Stokes equation for blood as Newtonian fluid

$$\rho\left[\frac{\partial v}{\partial t} + (\nabla v)\cdot v\right] = -\nabla p + \mu\cdot\Delta v \tag{2}$$

where v is the velocity, ρ is fluid density, p is pressure, μ denotes the kinematic viscosity of the fluid. We adopt assumption membrane balance law for the arterial wall equilibrium as

$$\frac{N_1}{R_1} + \frac{N_2}{R_2} + p = h\rho\frac{d^2w}{dt^2} \tag{3}$$

N_1 and N_2 denote the membrane stress resultants, R_1 and R_2 are principal radii of curvature blood vessel segment, w is displacement and h is wall thichnes. The surface pressure p comes from blood-wall complex interaction. The arteries tend to respond primarily in membrane mode rather than in bending mode, because the cardic pulse has a longe wavelength. The no slip condition on the fluid-wall interface is used as boundary condition

$$v = \frac{\partial u}{\partial t} \tag{4}$$

where u is wall displacement. It is convinient to parametrise the domain with a curvilinear coordinates, such as toroidal or helicoidal coordinates system (r, ϑ, z) as is shown by Figure 2.

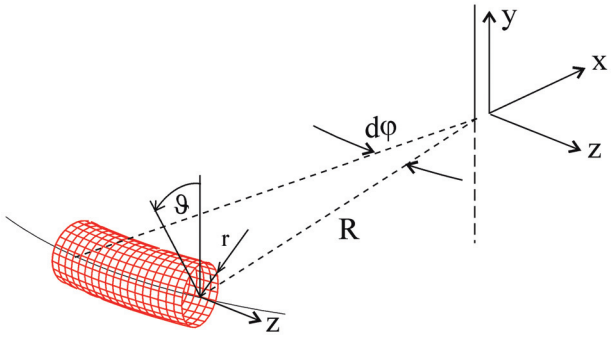

Fig. 2. Toroidal coordinate system.

The blood vessels overall geometry are represented by centarline curvature κ and torsion τ, diameter d and vessel segment lenght Δs. We shall consider the blood vessel curvature to be

$$\kappa = \kappa_0(1+\varepsilon\ \sin t) \tag{5}$$

Here κ_0 is the mean curvature and ε represent the small amplitude of its oscillations. It is well known that the vascular flow can be decomposed into a steady dominant part $\bar{\Pi}$ and an oscillatory component $\hat{\Pi}$ over it

$$\Pi(r,\vartheta,z,t)=\bar{\Pi}(r,\vartheta,z)+\hat{\Pi}(r,\vartheta)\cdot\exp\left[j(\omega t-kz)\right] \quad (6)$$

where ω is the circular frequency, k is wave number. The influence of the curvature κ and torsion τ on solution is analyzed by perturbation method, and therefore displacement and pressure we can write in the form of series expansions as follow

$$\begin{aligned}
\hat{u} &= u_0+\delta\kappa\cdot u_1+\delta\tau\cdot u_2+(\delta\kappa)^2\cdot u_3+(\delta\tau)^2\cdot u_4+..\\
\hat{v} &= v_0+\delta\kappa\cdot v_1+\delta\tau\cdot v_2+(\delta\kappa)^2\cdot v_3+(\delta\tau)^2\cdot v_4+..\\
\hat{w} &= w_0+\delta\kappa\cdot w_1+\delta\tau\cdot w_2+(\delta\kappa)^2\cdot w_3+(\delta\tau)^2\cdot w_4+..\\
\hat{p} &= p_0+\delta\kappa\cdot p_1+\delta\tau\cdot p_2+(\delta\kappa)^2\cdot p_3+(\delta\tau)^2\cdot p_4+..
\end{aligned} \quad (7)$$

where $\delta\kappa$ and $\delta\tau$ are small perturbations. In the asymptotic expansion $()_0$ corresponds to the axisymmetric solution in a straight tube, the Hagen-Poiseuille flow. The secondary flow phenomena under high pulsatile frequency are of great importance. The differential equations of various orders of $\delta\kappa$, $\delta\tau$ and $\delta\Omega$ can be obtained by substituting expansions (7) into the (1), (2), (3) and (4) equating the coefficient of various orders. The problem reduces to a linear system of ordinary differential equations[10]. Introducing the stream functions, Ψ the secondary flow is described by the following expressions

$$\frac{1}{R_S}\nabla^4\psi_0-\frac{1}{r}\left(\frac{\partial\psi_0}{\partial r}\frac{\partial}{\partial\vartheta}-\frac{\partial\psi_0}{\partial\vartheta}\frac{\partial}{\partial r}\right)\cdot\nabla^2\psi_0=0 \quad (8)$$

$$\begin{aligned}
&\frac{1}{R_S}\nabla^4\psi_1-\frac{1}{r}\left(\frac{\partial\psi_0}{\partial\vartheta}\frac{\partial}{\partial r}-\frac{\partial\psi_0}{\partial r}\frac{\partial}{\partial\vartheta}\right)\cdot\psi_1\\
&-\frac{1}{r}\left(\frac{\partial\psi_1}{\partial\vartheta}\frac{\partial}{\partial r}+\frac{\partial\psi_1}{\partial r}\frac{\partial}{\partial\vartheta}\right)\cdot\psi_0=0
\end{aligned} \quad (9)$$

where R_S is Reynolds number for secondary flow. The corresponding no-slip boundary condition for stream function ψ_0 and ψ_1 at $r=1$ are given by

$$\psi_0=0 \qquad \frac{\partial\psi_0}{\partial r}=\frac{1}{4}\sin\vartheta$$

$$\psi_1=0 \quad \frac{\partial\psi_1}{\partial r}=\frac{\sqrt{2}}{2}\cos\Phi\cdot\sin\vartheta$$

The additional symmetry conditions $\psi_0=\psi_1=0$ on the line $\vartheta=0$, π should be accounted in solution procedure. The equations (8) and (9) are numerically solved using the finite difference method for approximate solution partial differential equations. Once ψ_0 and ψ_1 have been found, the overall solution for the secondary streamfunction in the vessel is given by

$$\psi=R_S\psi_o+\alpha\varepsilon\cdot R_S^{1/2}\psi_1\cdot s \quad (10)$$

where s is the distance along the centreline of the vessel, α is Womersley number.

In order to characterize flow complexity, some flow descriptors are suggested. The kinetic helicity Ξ is proposed[4], as flow descriptor for the quantification spiral motion.

$$\Xi(x,t)=\frac{v\bullet(\nabla\times v)}{|v|\cdot|\nabla\times v|} \quad (11)$$

The wall shear stress[11] (WSS) is basic descriptor related to physiological fluid dynamics with high influence on development of atherogenesis. The components of the WSS τ_{rz} and $\tau_{\vartheta z}$ are as follow

$$\begin{aligned}
\tau_{\vartheta z} &= G\,\gamma_{\vartheta z}\\
\tau_{rz} &= G\,\gamma_{rz}
\end{aligned} \quad (12)$$

where γ_{rz} and $\gamma\vartheta_z$ are component of shear strain tensor, G is shear modulus of vascular wall. The oscillating shear stress index (OSI) is used to identify wall shear stress (WSS) values during the cardiac cycle on the vessel subjected to highly oscillating wall. These regions are usually associated with bifurcating flows and vortex formation that are strictly related to atherosclerotic plaque formation and fibrointimal hyperplasia. In accordance with Ku[2] the OSI can be defined as

$$OSI=\frac{1}{2}\left(1-\frac{\left|\int_0^T\tau_{xy}(x,t)dt\right|}{\int_0^T\tau_{xy}(x,t)dt}\right) \quad (13)$$

Experimental

A simplified model of a bifurcation as a replica of healthy human carotid artery with two branches known as Y-model analysed by some researches[8,11,12]. The parametric geometry defined by six parameters[14]; inflow diameter D, outflow diameters d_1, d_2 internal and external artery angles ϑ_1 and ϑ_2 and bulb position l, is illustrated in Figure 3. Non-Newtonian, blood-like fluid pulsatile flow across elastic rubber-like carotid artery model under physiological condition was studied. The Re=250 was used as average Reynolds number. The velocity distribution was measured with a laser-Doppler anemometer. The velocity curve used to the experiments is shown in Figure 3. An intravascular ultrasound (ivUS), angiographic or MRI (magnetic resonance image) is available technique to 3D reconstruct the blood vessel geometry in vivo. These techniques, in combination with computa-

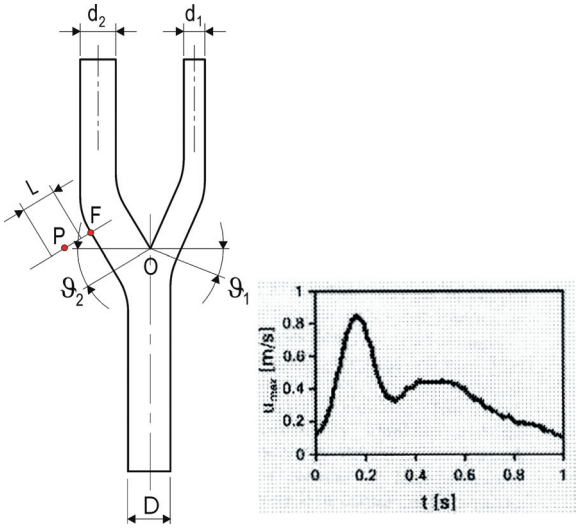

Fig. 3. The symmetric bifurcation with velocity pulse.

tional fluid dynamics (CFD), allow detailed patient-specific acquisition of local hemodynamics phenomena for clinical practice useful information[12].

Platelet deposition

The platelet deposition and thrombus formation has occurred in areas of normal flow directed toward the wall. Some study showed that circumferential plaque distribution depends on curvature of a bent vessel and vessel wall thickness. The use of axially symmetric stagnation point flow geometry for the investigation of thrombus growth under controlled conditions for varying thrombogenic surfaces. We assume that due to the relatively high shear rate in the domains of interest then blood can be modelled as a Newtonian fluid with constant temperature[15]. The multicomponent model for platelet transport by convection and diffusion with supposition a constant mixture density may be written

$$\frac{\partial c_i}{\partial t} + (v \cdot \nabla) c_i = \nabla (D_i \cdot \nabla c_i) + r_i \qquad i = 1, 2 \ldots, n \qquad (14)$$

c_i is the concentration i-th species, r_i is the reaction rate for the i-th species, D_i is the i-th species diffusion coefficient. We assume that Fickian diffusion model and activated platelets are the only issues of interest in modelling. The boundary condition for a reactive surface is formulated by equating mass diffusion at the wall with the platelet adhesive flux

$$D \frac{\partial c}{\partial n}\Big|_{wall} = k \cdot c_{wall} \qquad (15)$$

where n is a normal to the reacting surface, k is surface reaction rate. The Falkner-Skan flow[16] past wedge together equations (14) and (15) are solved by finite difference method (see Figure 4).

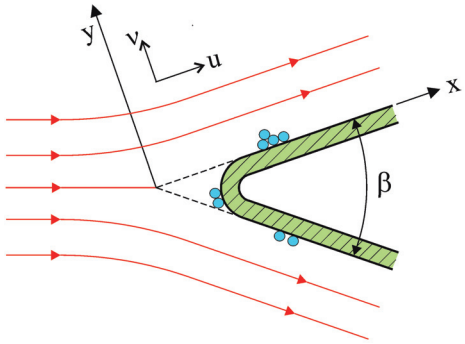

Fig. 4. Wedge boundary layer flow model.

Results

In order to illustrate time-dependent curvature on flow, Figure 5 shows leading-order streamline of secondary flow as the solution of above equations (8) and (9) at R_S = 0,100,250 respectively. As the value of Reynolds number increases, the vortex continues to be shifted in the direction of the flow, from the outside of the bend towards the inside.

On the other hand, in order to illustrate bifurcation complexity phenomena, Figure 6 shows the axial velocity distribution for several phases ωt = 0°, 60° and 120° over the pulse at the apex in internal carotid artery. The axial velocity profile in mother channel is symmetric and influence the branching in the neiborhoud. The presence of branching results in vortex skewing and loss of symmetry. The shift of the flow core towards the outside wall in the branch produces an overall rotating fluid motion.

When flow is diverted into the branch segment, it becomes inevitable for the flow to separate from the corner of the junction and a recirculation zone is formed. The sizes of the two recirculation zones depend on Reynolds number, flow diversion ratio (ratio of the flow rate through the side branches to the total flow rate). The flow separation development is followed by branching angle increases. The recirculation flow strongly influences the distribution of the shear stress. Another recirculation vortex may also appear along the outer wall of the main channel near the bifurcation region. Figure 7 shows the secondary flow distribution over cross section for several phases (ωt = 0°, 60°, 120°, respectively), over the pulse at the apex in internal carotid artery.

The wall shear stress (WSS) in curved vessel is dominated by its axial component. The curvature increases, the axial velocity is forced toward the outer wall and the secondary velocity field is increased in strength. The torsion skews the components of velocity in the direction of the increasing of the torsion. The non-uniform torsion induces skewed axial component of velocity with increased deformity in shape. For a vessel with a spiral centreline and uniform torsion WSS increases in magnitude. The WSS increases with torsion and increases in oscillatory manner. For constant curvature κ_0 = 0.09, and torsion which increases with distance s

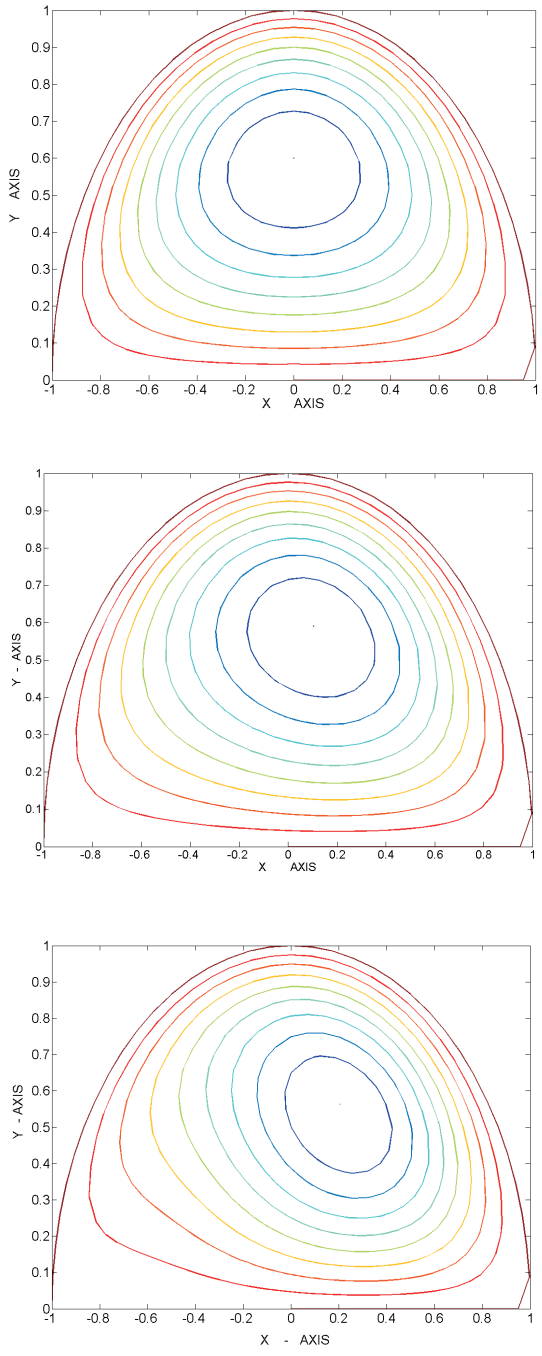

Fig. 5. a) Secondary stream function for R_S = 0. b) Secondary stream function for R_S = 100 c) Secondary stream function for R_S = 250.

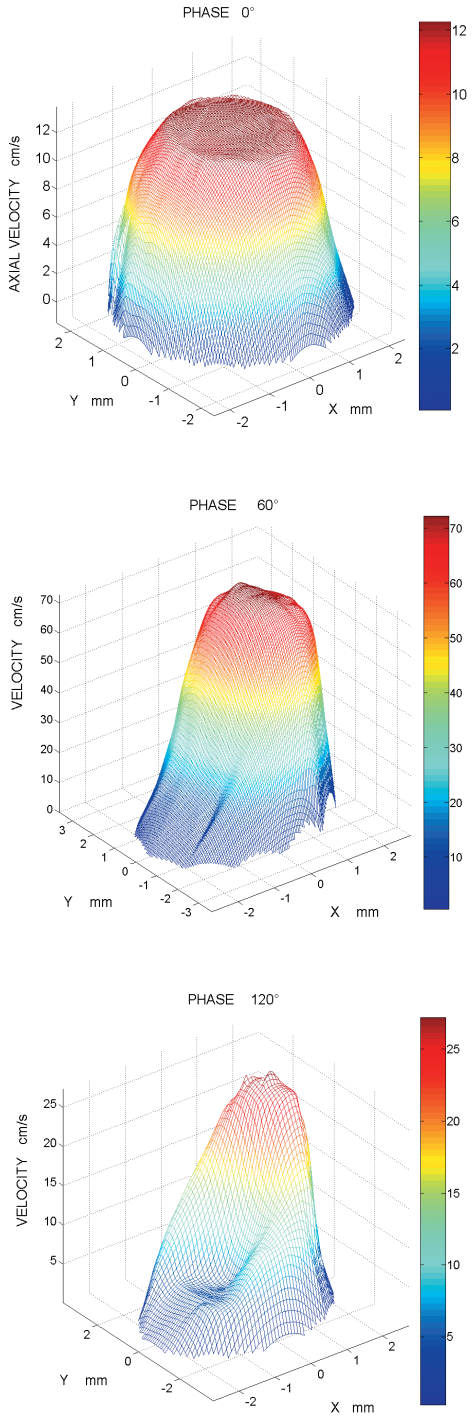

Fig. 6. a) Axial velocity distribution at apex, at phase 0°. b) Axial velocity distribution at apex, at phase 60°. c) Axial velocity distribution at apex, at phase 120°.

$$\tau = 0.1 \exp(0.1\ s)$$

on Figure 8 dimensionless wall shear stress ($\tau_{xy} = \tau_{xy} / \rho v^2_0$) dependence on circumference angle and torsion is shown. It suggests that adding a twist to a graft will reduce the possibility of plaque build-up. A new imaging technique was applied to study 3D plaque and shear stress distribution in artery bifurcation[12].

For this work, a domain 400 μm × 10 mm rectangular flow layer on wedge near branching was discretised. The following value for constants is;

$$D = 1.66 \times 10^{-7}\ cm^2/s$$

$$k = 4.6 \times 10^{-3}\ cm/s$$

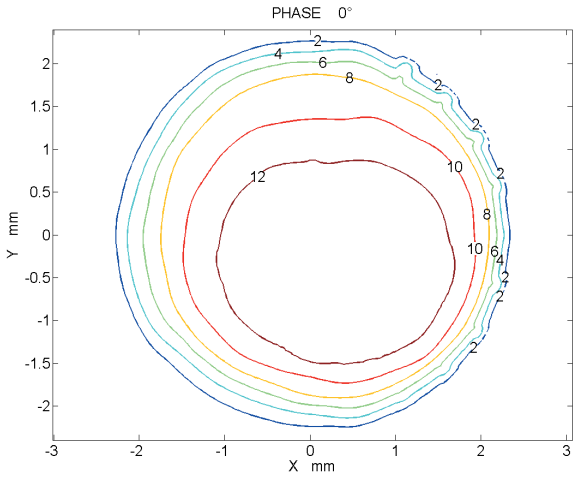

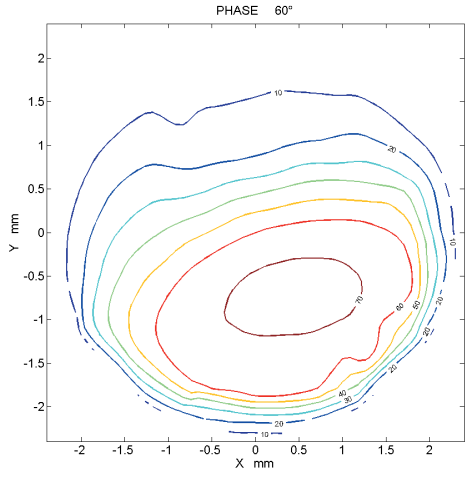

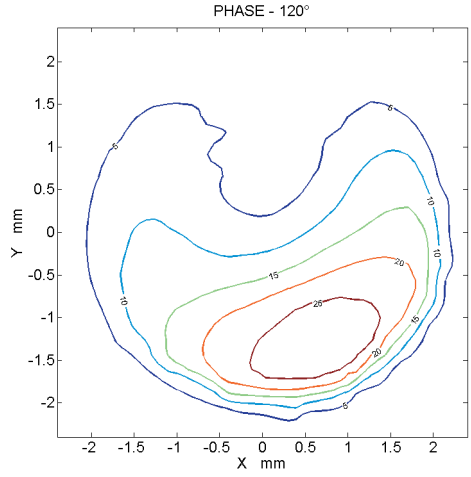

Fig. 7. a) The secondary flow distribution at the apex of branching at phase 0°. b) The secondary flow distribution at the apex of branching at phase 60° c) The secondary flow distribution at the apex of branching at phase 120°.

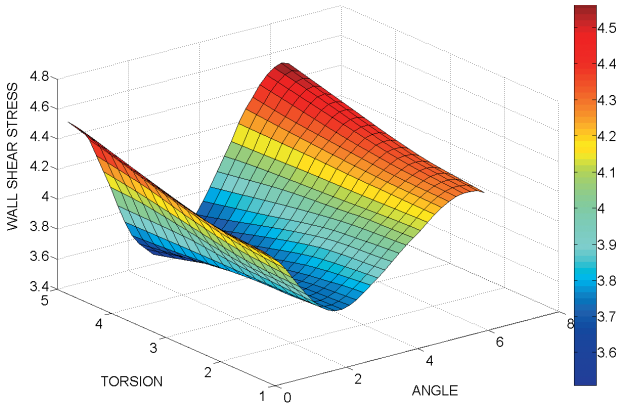

Fig. 8. Wall shear stress dependence on polar angle and torsion.

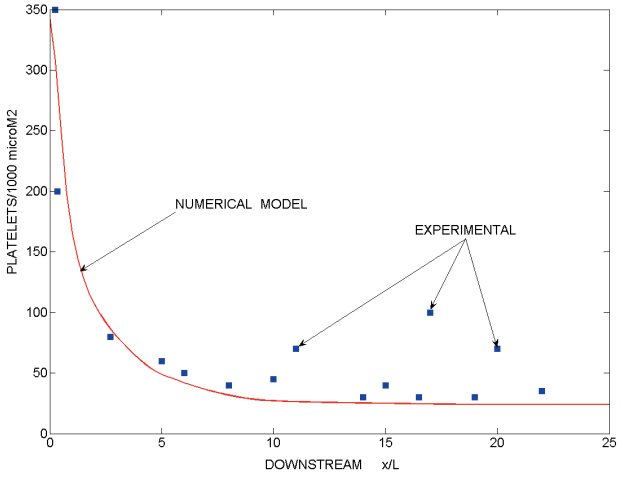

Fig. 9. Axial platelet deposition on downstream wedge surface.

The linear dependence diffusion constant on shear rate is assumed. The simulation is compared with experimental data[17]. Discrepancies between results (see Figure 9) come from simplified model and roughly estimated material constants.

Discussions

The vascular system is influenced by pulsatile load and a proper understanding behaviour of this system is based on studying localised dynamics blood flow effects. Dominant geometric influence factors on the flow are vessel time-dependent curvature and torsion, different branching angles and tube-diameter ratio.

Using perturbation analysis influence time-dependent curvature and torsion on secondary flow is illustrated by examples. Parametric dependence wall shear stress on torsion and curvature are obtained by approximate analytic method. Bifurcation phenomena illustrat-

ed by use experimental Y-model under pulsatile flow. The secondary flow structure influenced by phase position and geometry descriptors of the model. Multidimensional platelet deposition downstream problem on curved blood wall are numerically modelled and solved in transformed coordinate space as axisymetric boundary-layer over wedge. The multiscale blood flow problem in this work is overcome by using perturbation analysis to connect different material and time scale and by using numerical methods on the other hand to solve field problem at given scale.

Conclusion

Geometry plays the key role in determining the nature of hemodynamic patterns. The secondary flow in vivo models is markedly different from that observed in idealized geometry models. Advanced fluid mechanics in the near future can explain many phenomena through rigor theoretical models. The numerical solutions are only examples in generalized theoretical models. The construction vascular proteses and its use in clinical practise are useful place of application theoretical fluid mechanics models.

REFERENCES

1. CARO CD, FITZGERAL JM, SCHROTER GRC, Proc Roy Soc London B, 177 (1971) 109. — 2. KU DN, GIDDENS DP, ZARINS CK, GLAGOV S, Atherosclerosis, 5 (1985) 293. — 3. NIKOLIC V, HUDEC M, Principi i elementi biomehanike *[*In Croatian*]* (Skolska knjiga, Zagreb, 1986). — 4. MORBIDUCCI U, PONZINI R, GRIGIONI M, REDAELLI A, Journal of Biomechanics, 40 (2007) 519. — 5. JUNG J, HASSANEIN A, RLYCZKOWSKI RW, Annals Biomed Engrg, 34 (2006) 393. — 6. LIU Y, ZHANG L, WANG X, LIU WK, Int J Numer Meth Fluids, 46 (2004) 1237. — 7. LIU KW, LIU Y, FARRELLN D, ZHANG L, Comput Meth Appl Mech Engrg, 195 (2006) 1722. — 8. MIJOVIC B, LIEPSCH D, Technology and Health Care, 11 (2003) 115. — 9. GAMMACK D, HYDON PE, J Fluid Mechanics, 433 (2001) 357. — 10. PONTRELLI G, TATONE A, European Journal of Mechanics B/Fluids, 25 (2006) 987. — 11. PIVKIN IV, RICHARDSON PD, LAIDLAW DH, KARNIADAKIS GE, Journal of Biomechanics, 38 (2005) 1283. — 12. GIJSEN FJH, WENTZEL JJ, THURY A, LAMERS B, SCHUURBIERS JCH, PSERRUYS PW, STEEN AF, Journal of Biomechanics, (in press). — 13. AGIC A, NIKOLIC V, MIJOVIC B, Coll Anthropol, 30 (2006) 815. — 14. BRESSLOFF NW, Journal of Biomechanics, 11 (2006) 002. — 15. SORENSEN EN, BURGREEN GW, WAGNER WR, Ann Biomed Eng, 27 (1999) 436. — 16. OLAGUNJA DO, Int J Non-Linear Mechanics, 41 (2006) 825. — 17. SORENSEN EN, BURGREEN GW, WAGNER WR, Ann Biomed Eng, 27 (1999) 449. — 18. PIVKIN IV, RICHARDSON PD, KARNIADAKIS GE, PNAS, 14 (2006) 17164.

A. Agić

Faculty of Chemical Engineering and Technology, University of Zagreb, Marulićev trg 19, 10000 Zagreb, Croatia
e-mail: aagic@marie.fkit.hr

FENOMENI TEČENJA KRVI NA VIŠESTRUKOJ MATERIJALNOJ SKALI

SAŽETAK

Svrha i cilj ovog rada je utjecaj vremenski promjenljive geometrije (zakrivljenost, torzija, bifurkacija) I pulzirajuće prirode krvotoka na sekundarni tok, smično naprezanje i pojavu arterosklerozе. Problem je razmatran kao problem višestruke materijalne skale koristeći se teorijon perturbacione analizom i numeričkim metodama. Utjecaj zakrivljenosti i torzije na strukturu sekundarnog toka ilustrirana je primjerom. Bifurkacija i grananje analizirano je eksperimentalno koristeći Y-model. Utjecaj geometrije na model depozije plateleta na analiziran je koristeći numerički model i Falker-Skan model graničnog sloja.